Disconnect Between the Developing Eye and Craniofacial Prominences in the Avian Embryo

Jamil Jomaa[a], Jessica Martínez-Vargas[b], Shadya Essaili[a], Nida Haider[a], and John Abramyan[a]*

[a] Department of Natural Sciences, University of Michigan-Dearborn, Dearborn, Michigan, USA

[b] Departament de Vertebrats, Museu de Ciències Naturals de Barcelona, Barcelona, Spain

Author for correspondence*
John Abramyan
Department of Natural Sciences
University of Michigan-Dearborn
114 SFC Bldg.
4901 Evergreen Rd.
Dearborn, MI 48128
Phone: (313)593-5477
E-mail: abramyan@umich.edu

Abstract

In the amniote embryo, the upper jaw and nasal cavities form through coordinated outgrowth and fusion of craniofacial prominences. Adjacent to the embryonic prominences are the developing eyes, which abut the maxillary and lateral nasal prominences. The embryos of extant sauropsids (birds and nonavian reptiles) develop particularly large eyes in comparison to mammals, leading researchers to propose that the developing eye may facilitate outgrowth of prominences towards the midline in order to aid prominence fusion. To test this hypothesis, we performed unilateral and bilateral ablation of the developing eyes in chicken embryos, with the aim of evaluating subsequent prominence formation and fusion. Our analyses revealed minor interaction between the developing craniofacial prominences and the eyes, inconsequential to the fusion of the upper beak. At later developmental stages, the skull exhibited only localized effects from missing eyes, while geometric morphometrics revealed minimal effect on overall shape of the upper jaw when it develops without eyes. Our results indicate that the substantial size of the developing eyes in the chicken embryo exert little influence over the fusion of the craniofacial prominences, despite their effect on the size and shape of maxillary prominences and components of the skull.

Keywords: Craniofacial prominence, microphthalmia, anophthalmia, maxillary prominence, medial nasal prominence, lateral nasal prominence, frontonasal mass, chicken embryo

1. Introduction

One of the seminal moments in the embryonic development of amniotes is the fusion of craniofacial prominences, completing formation of the primary palate, upper lip and nasal cavities (Abramyan and Richman, 2015; Abramyan et al., 2015). A single frontonasal mass first forms in the midline and will eventually give rise to two medial nasal prominences, while the maxillary and lateral nasal prominences arise lateral to the embryonic oral cavity (stomodeum) shortly after (Fig. 1). As development progresses, the corners of the frontonasal mass (globular processes) fuse with the maxillary and lateral nasal prominences on both sides of the facial midline; simultaneously forming an intact upper lip/beak and nasal cavities (Abramyan et al., 2015). In the mature animal, lateral nasal prominences will eventually give rise to the nasal turbinates (MacDonald et al., 2004), the medial nasal prominences will form the nasal septum and premaxillary bones (Richman and Tickle, 1989; Wedden, 1987), and the maxillary prominences will give rise to the maxillary and palatine bones (Lee et al., 2004).

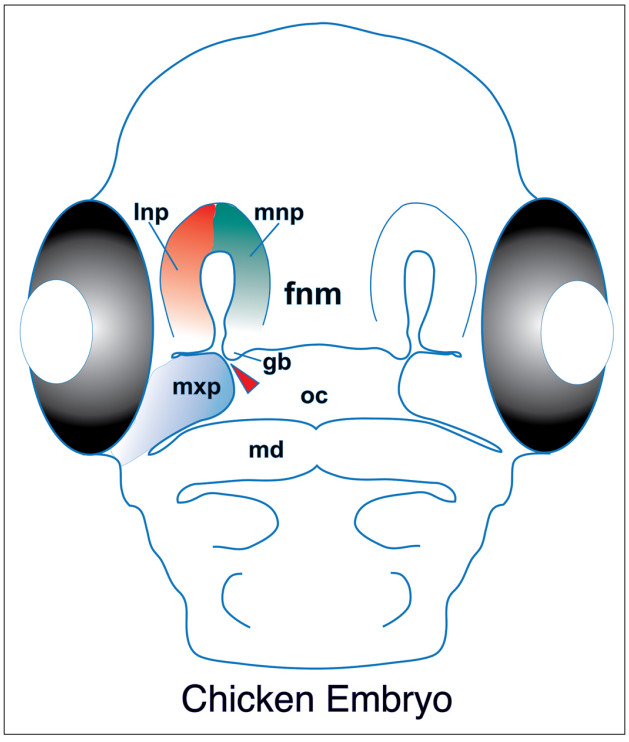

Fig. 1. Illustration of a stage 28 chicken embryo. Red arrowhead indicates the point of fusion between the maxillary prominence and the globular process of the frontonasal mass. fnm, frontonasal mass; gb, globular process; lnp, lateral nasal prominence; md, mandibular prominence; mnp, medial nasal prominence; mxp, maxillary prominence; oc, oral cavity.

Around the same period that the craniofacial prominences form, the embryonic eyes begin to develop adjacent to the maxillary and lateral nasal prominences (Abramyan and Richman, 2015).

Possibly due to the small size of the eyes in the mammalian embryo (Jeffery et al., 2002), the potential influence of the developing eye on early craniofacial prominence patterning has received little attention. The eyes in embryonic sauropsids (birds and nonavian reptiles), on the other hand, are significantly larger and directly abut the maxillary and lateral nasal prominences (Abramyan et al., 2015; Jeffery et al., 2002). This is particularly evident in the chicken embryo (*Gallus gallus*), where the placement of the eyes suggests a greater likelihood that they may influence prominence morphology, outgrowth, and/or fusion. Due to their position and substantial size, authors have previously hypothesized that the eyes may influence developing prominences during the fusion of the upper beak either through molecular communication or through a strictly physical effect (Abramyan et al., 2015; Parsons et al., 2011).

Occasionally, chicken embryos in the laboratory will develop microphthalmia or anophthalmia, where the eye is abnormally small or malformed in the former, and completely missing in the latter (Bellairs, 1955; Coulombre and Crelin, 1958; Landauer, 1938). However, these specimens are not usually considered for further scientific analysis after identification, with no mention of clefting or timeline of fusion recorded in the literature. That said, a number of studies have explored the role of the eye on the later morphogenesis of the skull, finding that orbital size, as well as position, size, and shape of individual bones surrounding the orbit are influenced by the size of the eye (Apt and Isenberg, 1973; Coulombre and Crelin, 1958; Dufton et al., 2012; Sarnat and Shanedling, 1974; Yamamoto et al., 2003). In experiments performed on chicken and rabbit embryos, studies have found that orbital size increases mechanistically due to increasing eye size (Coulombre and Crelin, 1958; Sarnat and Shanedling, 1974). Perhaps not unexpected, the opposite effect occurs after enucleation (Apt and Isenberg, 1973), or even simply lens removal, which results in a smaller eye size and concomitant changes in the orbital bones (Dufton et al., 2012). In fact, prosthetic eyes are currently used in children with anophthalmia in order to facilitate normal shape in the developing orbit and skull (Gundlach et al., 2005; Tucker et al., 1995).

Anophthalmia and microphthalmia have also been found to affect the skeleton of the developing jaw in the chicken embryo. In one of the earlier publications on the topic, Landauer recognized developmental abnormalities in the eye as a primary cause for the “cross-beak” condition in

developing chickens, where the upper beak turns towards the side of the missing or abnormal eye (Landauer, 1938). Subsequent to this work, several authors have performed more detailed analyses of the condition in the chicken model by experimentally reducing eye size and characterizing the resulting skeletal malformations (Apt and Isenberg, 1973; Coulombre and Crelin, 1958; Sarnat and Shanedling, 1974; Yamamoto et al., 2003). However, these studies focus on descriptive analyses of the ossified skull, with no mention of the craniofacial prominences or influence on early craniofacial patterning, which remain largely unexplored.

The purpose of this study was to fill this gap in knowledge and assess whether the developing embryonic eyes exert any influence over the development and morphology of craniofacial prominences at early embryonic stages, using the chicken embryo as a model. By performing complete ablation of the embryonic eye primordium prior to the formation of the craniofacial prominences (stages 16-18, unless note otherwise), we analyzed the development of the prominences, as well as primary palate, without the presence of the eye. This methodology differs from earlier studies comprised of either incomplete removal of the eye (leading to partial regrowth) (Bellairs, 1955) or simply reduction in size (Coulombre and Crelin, 1958); both methods still retaining ocular tissue that could potentially send molecular signals to the developing prominences. The embryos resulting from our experiments exhibited complete anophthalmia, along with minimal disruption to the shape of the developing prominences, with no cases of cleft beak, and only one instance of delayed fusion observed. At later stages of development, the ossified skull did exhibit both local and general changes in shape due to the missing eye, as previously reported by Coulombre and Crelin (1958) and Landauer (1938). Taken together, our results demonstrate a relatively minor role for the eyes in early craniofacial patterning, with increasing significance as the embryo matures.

2. Results

2.1. Difference in Embryonic Eye Size

In order to highlight the considerable disparity in relative eye size between murine and avian embryo during primary palate fusion, we performed segmentation analysis at stage 28 in chicken (Sun et al., 2000) and E12 mouse (Jiang et al., 2006), as well as the subsequent developmental stage, where fusion is complete (stage 29 in chicken and E13 in mouse). Segmentation of microCT scanned heads revealed that each eye occupies 7.9 ± 0.6% and 11.2 ± 1.5% of total head volume in stage 28 and 29 chicken embryos respectively, while only occupying 0.2 ± 0.04% and 0.35 ± 0.04% of head volume in E12 and E13 mouse embryos (Fig. 2A-C). There was no significant difference between the left and right eye in chicken or mouse samples at any stage (data not shown).

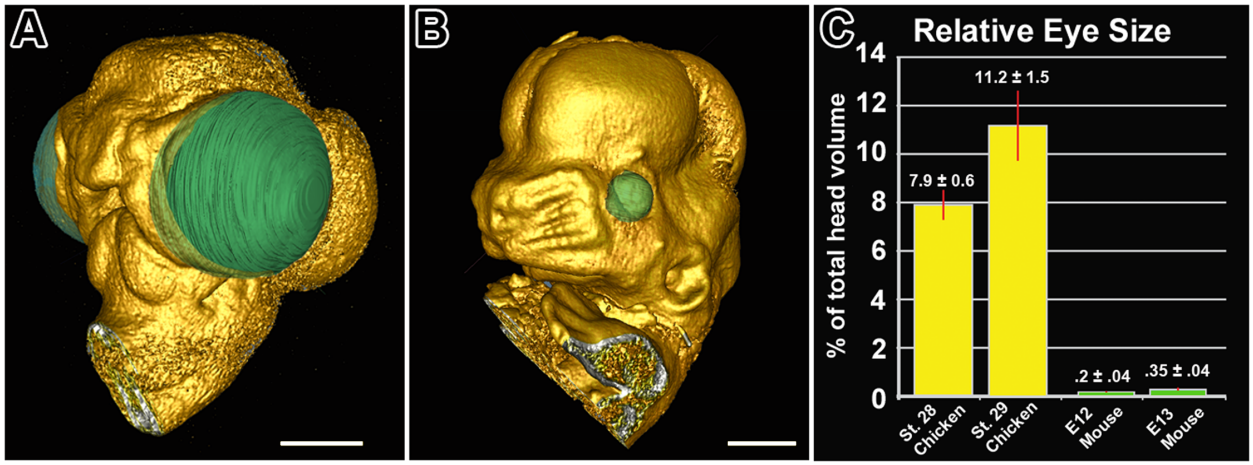

Fig. 2. Comparison of relative eye size between chicken and mouse at similar embryonic stages. MicroCT scans of representative stage 29 chicken embryo (**A**) and representative E13 mouse embryo (**B**) with eye segmented. (**C**) Graph depicting relative eye size in chicken in comparison to mouse. Both eyes from chicken and mouse were averaged for final value since left and right side did not exhibit significant difference in size. Scale bars: 1.5 mm

2.2. Effect of Eye Ablation on Position and Fusion of Craniofacial Prominences

Unilateral ablation of the eye primordium was performed prior to prominence formation, and assessed for defects in downstream craniofacial development and patterning (Fig. 3). The control side exhibited normal eye development, while the contralateral treated side left a concave depression in the area where the eye was removed (Fig. 3A, B – red arrowheads). The primary palate appeared relatively normal on both sides of the midline (Fig. 3C,C'). Analysis of cross sections through the primary palate also revealed comparable morphology of craniofacial prominences on both sides of the face (Fig. 3D-G).

When prominence volume was analyzed, the maxillary prominence was consistently smaller on the anophthalmic side when compared to the contralateral control at the time of fusion (stage 28) $p = 0.0014$ (Fig. 3H,I). There also appeared to be a visible difference in shape of the globular processes. When the globular process was analyzed, the process on the anophthalmic side was consistently larger than on the contralateral control side, although the difference was not statistically significant, $p = 0.06$ (Fig. 3J,K). The difference in sizes led us to suspect that the anophthalmic side may exhibit a delay in fusion, and inspection of the isosurface renderings initially seemed to support this idea. However, when we examined cross-sectional views from the microCT scans through the fusion zone in stage 28 animals (9 from specimens where anophthalmia surgeries were performed at stage 16-18 and 5 from surgeries performed at stage 13-14), we observed only one specimen from the latter group where the microphthalmic side remained unfused while the control side was fused, in contrast to bilateral fusion in the rest. Thus, there appeared to be no tangible delay in fusion, despite the size and shape difference of the maxillary prominences.

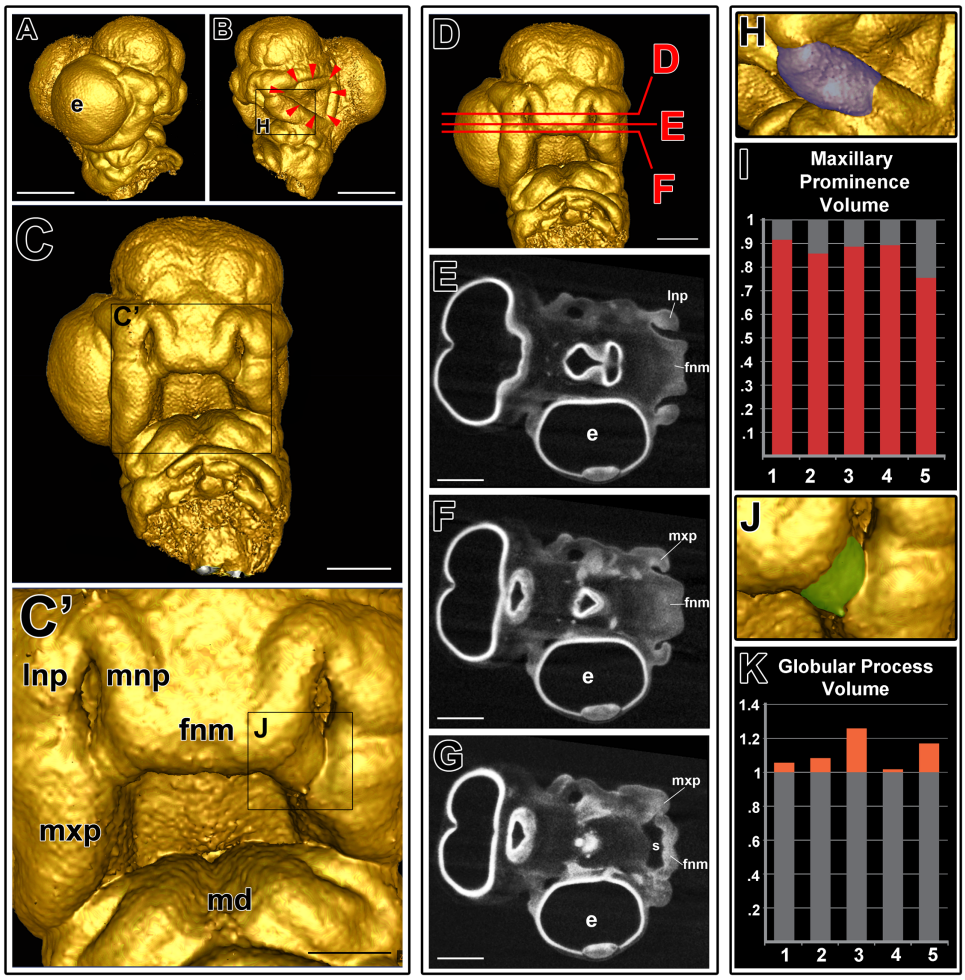

Fig. 3. Representative stage 28 chicken embryo with normal fusion of the primary palate. (**A**) Control side of embryo with normal eye formation. (**B**) Anophthalmic side of the embryonic head revealing the depression resulting from eye ablation (red arrowheads). (**C**) Frontal view of embryo revealing morphological disparity in the eye region between the left and right sides, with relatively normal primary palate formation. **(C')** Magnified view of embryonic face showing fusion between the fnm and the mx. (**D-G**) Digital cross sections in the transverse plane from microCT scans of stage 29 embryo revealing normal morphology of the lnp and mxp, with fusion evident between the fnm and mxp in panel **(G)**, forming an intact primary palate. (**H-I**) Volumetric analysis of segmented maxillary prominences from representative stage 28 embryos reveals a consistent, significantly smaller volume in the treated side (red) as compared to respective control side (gray), p = 0.0014 (n=5). (**J-K**) Volumetric analysis of segmented globular process from representative stage 28 embryos reveals a consistently larger volume in the treated side (orange) as compared to respective control side (gray) (albeit non-significant, p = 0.06) (n=5). e, eye; fnm, frontonasal mass; mxp, maxillary prominence; lnp, lateral nasal prominence; md, mandibular prominence; s, stomodeum. Scale bars: A,B - 2 mm, C - 1mm, C' - 0.5mm, D-F - 1mm

2.3. Effect of Eye Ablation on Craniofacial Prominence Shape After Fusion is Complete

When the lateral nasal and maxillary prominences were analyzed in stage 29 animals, we still observed differences in shape between the anophthalmic and control sides (Fig. 4). While the difference in volume described at stage 28 was sufficiently minimal as to not affect beak fusion itself, the anophthalmic side remained significantly more rounded in comparison to the flatter, contralateral control, even after the primary palate was fused (Fig. 4B'; Table 1).

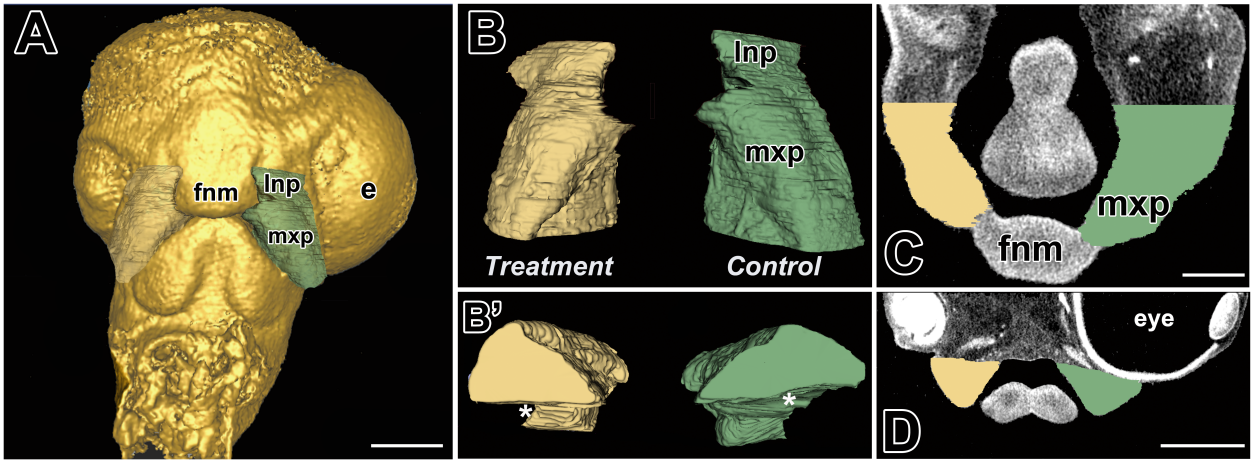

Fig. 4. Segmentation of lateral nasal and maxillary prominences in stage 29 chicken embryo with unilateral anophthalmia. Segmentation reveals similar morphology from a frontal, exterior view of prominences (**A** and **B**). (**B'-D**) Cross sections from the caudal-posterior (**B'**) as well as transverse (**C**) and frontal (**D**) planes reveal flatter and wider shape of maxillary prominence on the control side, while the treated side narrows and increases in height (**B'**). (**B'**) Asterisks indicate dorsal side where prominence abuts the eye. e, eye; fnm, frontonasal mass; mxp, maxillary prominence; lnp, lateral nasal prominence. Scale bars: A - 1 mm, C - 0.5 mm, D - 1mm

Table 1. Maxillary prominence roundedness score

	Control - mxp	Treatment - mxp	p-value
Cranial	0.65	0.69	0.00211
Middle	0.63	0.77	**<0.00001**
Caudal	0.56	0.75	**<0.00001**

*Values closer to 1 indicate more rounded shape

2.4. Effect of Eye Ablation on the Developing Skull

Unilateral anophthalmia induction in the chicken embryo produced a similar skull phenotype to severely microphthalmic embryos described in earlier studies (Coulombre and Crelin, 1958; Sarnat and Shanedling, 1974). Therefore, we will only provide a brief overview of the resulting phenotype, in the interest of clarifying our subsequent morphometric analyses. All unilaterally anophthalmic embryos exhibited deviation of the upper beak towards the treated side (Fig. 5C) (Coulombre and Crelin, 1958; Landauer, 1938). This phenotype is associated with a smaller orbit on the anophthalmic side (Fig. 5A, B) and changes in the shape of the surrounding frontal, jugal, and quadratojugal bones (Fig. 5C, D). From a palatal view, we observed shortening of the jugal and quadratojugal on the anophthalmic side, while contralateral bones bowed outwards to accommodate the deviation (Fig. 5D). We furthermore analyzed shape change in the larger bones in the palate: premaxilla, maxillary, palatine and pterygoid. We compared differences in surface area between the microphthalmic side and the contralateral control side of these bones and found that the palatine and pterygoid both exhibit significant differences in area between the microphthalmic and control sides (Supplementary Fig. S1, Supplementary Table S1).

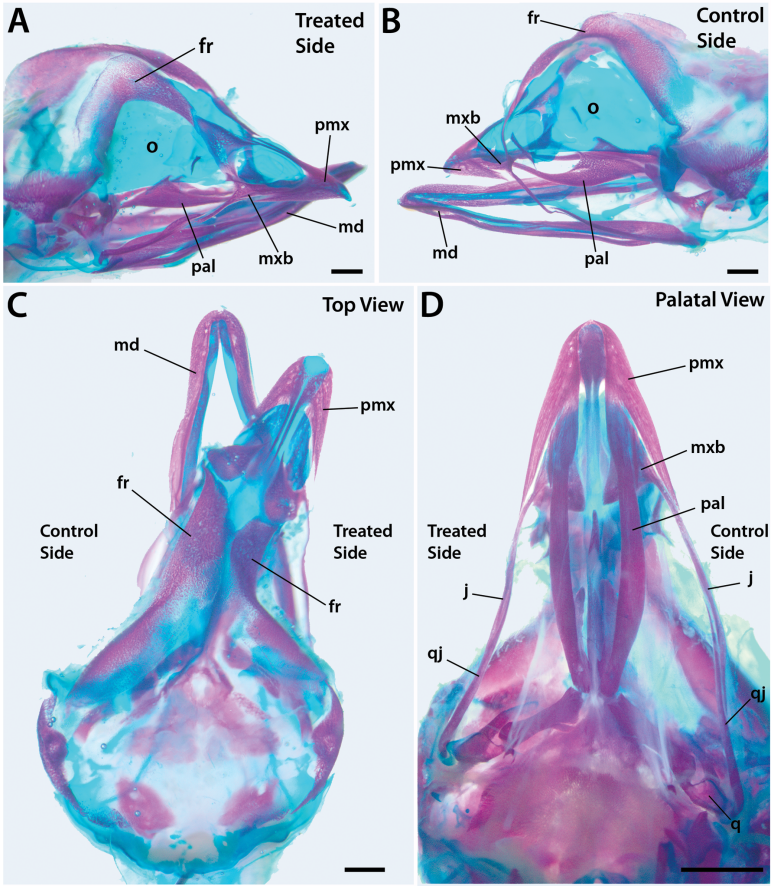

Fig. 5. Cleared and stained skeletal preparation of stage 41 chicken embryo with unilateral eye ablation. (**A**) Treated side of embryo reveals a thickened and shortened frontal bone, which reduced the size of the orbit as compared to the control side with a normal eye (which has been removed) (**B**). (**C**) Dorsal view of skull revealed a significant deviation of the upper beak towards the anophthalmic side (treated side), while the mandible remains straight. (**D**) Palatal view of embryo revealed shortening of the treated side as compared to the normal side. fr, frontal; j, jugal; md, mandible; mxb, maxillary bone; o, orbit; pal, palatine bone; pmx, premaxilla; q, quadrate; qj, quadratojugal. Scale bars: 1.0 mm

2.5. Novel Insights into Skull Shape in Anophthalmic Embryos

In order to obtain a more comprehensive understanding of how skull shape is affected by the eyes in the avian embryo, we performed 2D geometric morphometric analyses on the palatal shape of samples (including additional unilateral samples ablated at stage 13-14). PCA revealed that PC1 and PC2 encompass 88.092% of shape variation. A scatter plot showed control specimens close to the origin of coordinates in a tight group, within the distribution of bilaterally anophthalmic specimens, while the two unilaterally ablated samples overlapped in distribution (Fig. 6B). Unilaterally and bilaterally anophthalmic samples exhibited the greatest degree of variance along both PC1 and PC2 axes, differentiating largely along PC1. The CVA scatter plot accounted for 98.08% of the variation in CV1 and CV2 among phenotypes scaled for within-group variation. CVA found both control and bilaterally treated samples aligned along CV1, clearly separated from both unilaterally anophthalmic samples (Fig. 6C). The shape changes associated with PC1 and CV1 consisted of anterior and posterior shifts of landmarks, primarily associated with shortening of the jugal and quadratojugal in unilaterally anophthalmic embryos on the right side of the palate, and lengthening on the contralateral side (Figs. 6D and 6F). PC2 accounted for lateral or medial shifts of landmarks along the sagittal midline (Fig. 6E), while shape changes linked to CV2 were barely noticeable. Procrustes distance calculation from CVA between control and bilaterally anophthalmic samples was 0.0087 ($p = 0.5013$), and 0.0137 ($P= 0.2020$) between specimens where anophthalmia was induced at stage 13-14 and stage 16-18. Larger and statistically significant Procrustes distances occurred between bilaterally and unilaterally anophthalmic samples (0.1070, $P < 0.0001$), as well as between control and unilaterally anophthalmic samples (0.1065, $P < 0.0001$).

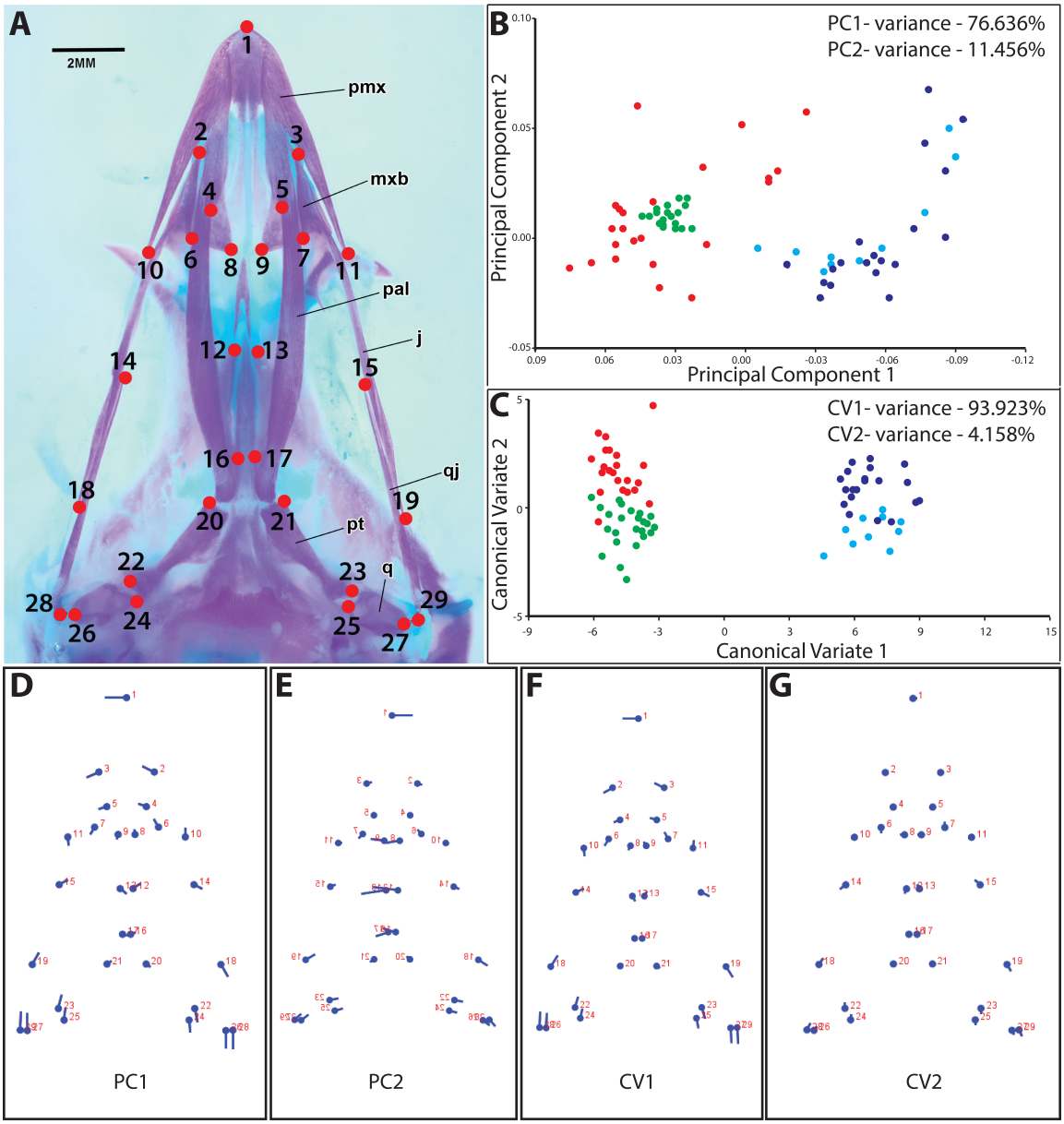

Fig. 6. (**A**) Palatal view of a control specimen displaying the layout of the 29 landmarks digitized (for anatomical definitions see Table 2). (**B-C**) Scatter plots of PC1 vs. PC2 scores and CV1 vs. CV2 scores according to phenotype (green – control (n=24); dark blue – unilateral stage 16-18 (n=20); light blue – unilateral stage 13-14 (n=10); red – bilateral (n=22)). Percentages of total variance for which the PCs account, and percentages of variation among groups scaled for the within-group variation explained by the CVs, are displayed. (**D-G**) "Lollipop" diagrams showing the shape changes associated with each PC and CV. Scale factors: -0.1 units (PC1 and PC2 shape change graphs) in negative direction, and 10.0 units (CV1 and CV2 shape change graphs) in positive direction from the consensus which corresponds to the dots in the diagrams and to the origin of coordinates in the scatter plots. j, jugal; mxb, maxillary bone; pal, palatine bone; pmx, premaxilla; pt, pterygoid; q, quadrate; qj, quadratojugal.

Diagrams resulting from Discriminant Function Analysis (DFA) highlighted the shape differences between the means of control and unilaterally anophthalmic samples, and between the means of bilaterally and unilaterally anophthalmic samples, with near identical shifts in landmark positions (Figs. 7A and 7B). Shape changes are mostly in the premaxilla, jugal, quadratojugal, and the quadratojugal's attachment point, the quadrate. In contrast, we observed no apparent change in landmark positions between the means of control and bilaterally anophthalmic phenotypes (Fig. 7C) or the two unilaterally anophthalmic sample groups (Fig. 7D).

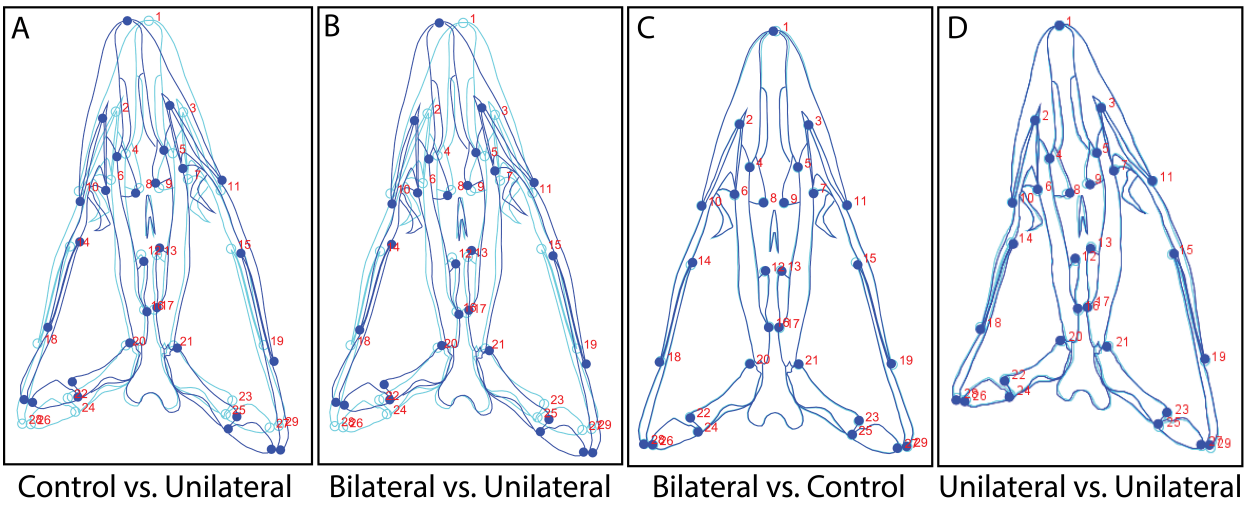

Fig. 7. Discriminant Function Analysis (DFA) warped outline diagrams showing the shape differences between the means of (**A**) control and unilateral, (**B**) bilateral and unilateral, (**C**) bilateral and control, and (**D**) stage 13-14 treated unilateral and stage 16-18 treated unilateral samples. Mean shape in light blue corresponds to the first phenotype mentioned in each comparison.

Additionally, no significant variation in the size of the entire palate was observed between all three phenotypes ($F = 1.662$, $p = 0.198$). However, when comparing the palatal area that comprised the orbit between the left eye of control and the remaining eye of unilaterally treated samples, a significant difference was found ($F = 8.752$, $p = 0.005$). The area measured in the remaining eye of anophthalmic samples was greater than that of the left eyes in controls, indicating enlargement of the control orbit in unilaterally anophthalmic samples.

2.6. Disruption in Laterosphenoid Patterning

The laterosphenoid bone normally contains the *foramen n. ophthalmici* (Baumel and Witmer, 1993; Clark et al., 1993), through which cranial nerve V1 (ophthalmic nerve) travels (Clark et al., 1993). Anophthalmic animals exhibited a distinct lack (or severe reduction in size) of *foramen n. ophthalmici* in the orbit where the eye was removed, while the contralateral (control) side of unilaterally anophthalmic animals exhibited normal morphology (n=11) (Fig. 7). Control specimens exhibited normal *foramen n. ophthalmici* in both laterosphenoid bones (n=20).

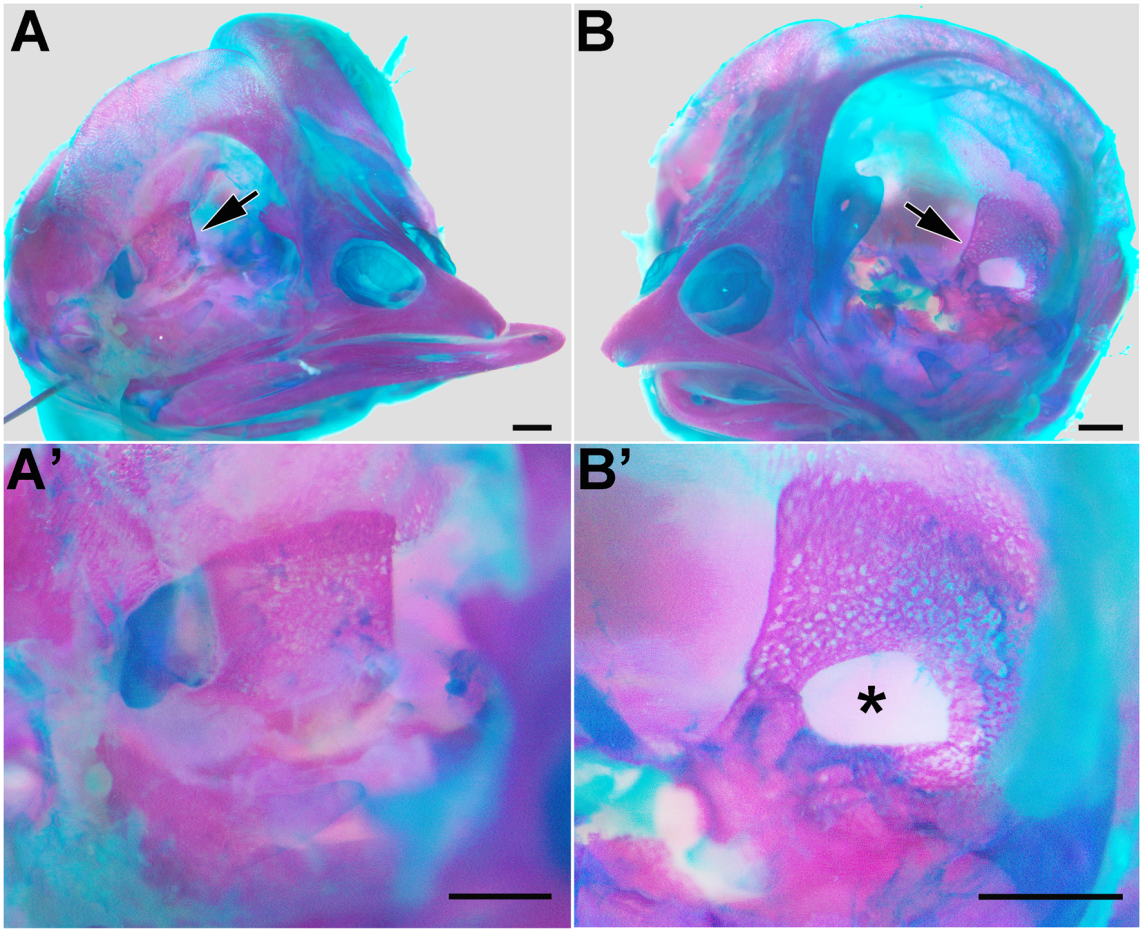

Fig. 8. Unilaterally treated sample reveals no visible foramen in the laterosphenoid on the treated side of the skull (**A**, **A'**). The control side (**B**, **B'**) displays the *foramen n. ophthalmici* through which the ophthalmic nerve passes (asterisk in **B'**). Scale bars: 1.0 mm.

3. Discussion

Fusion of the primary palate is a shared developmental milestone across amniotes, and represents a critical step in development due to the substantial risk of developing a cleft in the lip or palate (Dixon et al., 2011). In the avian embryo, fusion takes place directly abutting remarkably large eyes that may influence not only prominence outgrowth, but also shape and fusion. Conversely, mammals possess smaller eyes through the majority of the embryonic developmental period. The dimensions of the embryonic eyes in birds have led a number of authors to examine the role of the eye on craniofacial development, focusing largely on skeletogenesis and morphology of individual bones of the skull (Bellairs, 1955; Coulombre and Crelin, 1958; Landauer, 1938). Yet earlier stages of development, including interaction of the craniofacial prominences with the developing eye, have received much less attention. Elucidating these early stages is important towards attaining a better understanding of the interaction between components of the embryonic face.

3.1. Prominence Outgrowth and Fusion After Eye Ablation

Since we removed the eyes at very early stages, prominence formation and outgrowth occurred entirely in their absence. Nonetheless, the maxillary and lateral nasal prominences developed in their appropriate positions and went on to perform their respective functions without much deviation. This occurs despite the smaller maxillary prominence on the anophthalmic side at the time of fusion. Even after fusion completed, the maxillary prominences on the anophthalmic side remained more rounded, likely due to relief from the mechanistic effects that such a large eye normally exerts on the dorsal surface of the developing prominence.

The reason that craniofacial prominence development and patterning is so robust may be attributed to intrinsic developmental instructions from their neural crest cell-derived mesenchyme. Prior to prominence formation, neural crest cells from the midbrain and anterior hindbrain migrate into the frontonasal, maxillary, and mandibular primordia (Couly et al., 2002; Couly et al., 1998). Through a long history of neural crest cell transplantation experiments performed on frogs, salamanders, fish, as well as a number of avian species including ducks and emus, scientists have confirmed that cranial neural crest cells control size, timing, and growth rate of the craniofacial complex (Schneider, 2018). For example, when neural crest cells from

quail were introduced into duck embryos, the ducks developed smaller, pointed beaks resembling that of the quail donor (Eames and Schneider, 2008; Fish et al., 2014; Schneider and Helms, 2003; Tucker and Lumsden, 2004). This underlying neural crest cell-directed patterning likely drives correct prominence formation, despite the lack of the adjacent eye. An alternative explanation may involve a compensatory mechanism by the prominences to correct any deviation which eye ablation may have caused. Fish and colleagues have found that compensation by neural crest cells is possible in cases where pre-migratory neural crest cells were extirpated (Fish et al., 2014). However, we do not believe this mechanism would be triggered since neural crest cell migration was complete by the time surgeries were performed. Taken together, our findings highlight a surprisingly robust system in the formation and eventual fusion of the primary palate, with minimal influence from the developing eye.

3.2. Eye Size Disparity Between Embryonic Reptiles and Mammals

When we quantified the disparity in relative eye size between embryonic birds and mammals, we found a substantial difference. Even in the tarsier, which possesses one of the largest eye-to-body mass ratios of any mammal, embryonic eye size is comparable to other mammals (Jeffery et al., 2002). This disparity has been previously recognized but not quantified, with delay in mammalian eye development thought to be the underlying cause (Bininda-Emonds et al., 2003; Jeffery et al., 2002). In embryonic mice, growth of the eye is slow until approximately E16 (past the period of prominence formation and primary palate fusion), after which a drastic growth increase is observed (Foster et al., 2003). This pattern is essentially reversed in the chicken embryo where two main growth phases take place. The first rapid phase occurs between stages 23 - 26 (days 4 - 5), while a second slower phase occurs between embryonic stages 36 - 42 (days 10 - 16) (Goodall et al., 2009; Kim et al., 2011; Neath et al., 1991). These studies influenced our methodology in deciding to perform eye ablation before the first period of avian optic growth, in order to minimize the influence of the ocular tissue on craniofacial prominence formation. Moreover, our analyses also revealed an increase in relative eye size as both mouse and chicken progressed in developmental stages, suggesting a more intricate relationship between eye size and developmental progression that remains to be explored.

3.3. Relationship Between the Eye and Developing Skull

Since the early 20th century, the eye has been suspected of having an effect on the formation of the vertebrate skull (De Beer, 1937). In humans, developmental syndromes that include microphthalmia and anophthalmia as part of their profiles often include serious malformation in the surrounding bony structures (Bardakjian and Schneider, 2011; Llorente-Gonzalez et al., 2011; Ng et al., 2002; Uz et al., 2010; Williamson and FitzPatrick, 2014), and often require prostheses in order to facilitate normal orbit and skull formation (Gundlach et al., 2005; Tucker et al., 1995). Accompanying these observations, a series of studies have looked at this question in a variety of organisms. Coulombre and Crelin used an intubation technique to drain vitreous fluid from the developing eye of the chicken embryo, thereby making it smaller in size; ultimately causing a beak deviation towards the smaller eye due to shortening of the "quadratojugomaxillary complex" (Coulombre and Crelin, 1958). This phenotype was replicated in our unilaterally anophthalmic samples. As the eye develops in the chicken embryo, its growth surpasses that of the independently growing orbit, mechanically increasing the size of the orbit (Coulombre and Crelin, 1958). Studies using the Mexican tetra (*Astyanax mexicanus*), which has naturally occurring blind cave populations as well as sighted surface populations, also demonstrate a relationship between the developing eye and the surrounding orbital bones (Dufton et al., 2012; Jeffery et al., 2002). Similar results were also obtained in mammalian studies, where unilaterally enucleated sheep exhibited a 35% decrease in orbit volume (Apt and Isenberg, 1973), while postnatal rabbits showed an increase in orbital size when silicone was injected into the eye (Sarnat and Shanedling, 1974). The aforementioned studies, coupled with work on chicken by others and us clearly showed that the size of the orbit and the shape and size of surrounding bones are susceptible to influence from the developing eye. The differences in the individual palatal bones that we observed were likely due to the deviation of the beak caused by unilateral anophthalmia, rather than specific influence of the eye itself.

Our initial analyses were performed on specimens where anophthalmia was induced at stage 16-18, after the optic cup has already formed and may have influenced the surrounding neural crest cells prior to anophthalmia induction. Therefore, we repeated the morphometric experiments with specimens where unilateral anophthalmia was induced at stages 13-14 (Thompson et al.,

2010). However, we found no significant difference between the specimens where unilateral anophthalmia was induced at stages 13-14, as opposed to stages 16-18, in any of our analyses.

When we performed morphometric analysis of the palatal view of the upper jaw, we found that besides the dramatic beak deviation in unilaterally anophthalmic animals, the embryonic eyes do not exert a disproportionate influence on the overall shape of the upper jaw when anophthalmia is bilateral. Geometric morphometrics revealed evident separation between the unilaterally anophthalmic specimens and the control and bilaterally anophthalmic specimens. As evident from the horizontal PC1 and CV1 axes, bilaterally anophthalmic and control specimens have an overlapped distribution, which indicates that, according to the shape features considered in PC1 and CV1, they are indiscernible. Moreover, PC1 and CV1 account for the majority of the variation in each case (~77% and ~94% respectively). PCA and CVA calculations do appear to show some difference between the control and bilaterally anophthalmic specimens in PC2 and CV2 (vertical axis), with a more noticeable difference in CVA likely because CVA assumes a priori knowledge of group membership, as opposed to PCA. Furthermore, PC2 only explains ~11.5% of total variation, while the CV2 axis explains only ~4% of variation among groups scaled for the within-group variation. Therefore, when displaying the differences between group means through DFA, it is not surprising that the mean shapes of bilateral and control samples are almost identical.

3.4. Interconnectivity Between the Developing Eye and Laterosphenoid

In the posterocaudal region of the avian orbit, a small bone called the laterosphenoid (Baumel and Witmer, 1993) (also sometimes referred to as the alisphenoid or orbitosphenoid in the literature (Hogg, 1978)) exhibited reduced or absent foramen for cranial nerve V1 in anophthalmic specimens. Cranial foramina allow nerves and associated blood vessels to pass through the skull (Akbareian et al., 2015). Akbareian et al. have demonstrated a correlation between the shape of blood vessels and the resulting foramina in chickens (Akbareian et al., 2015). By removing the eye, we likely eliminated the developing ophthalmic nerve and its associated blood vessels. Thus, nothing prevented complete or near-complete closure of the *foramen n. ophthalmici* in anophthalmic chicken embryos.

3.5. Conclusions

If the eye did indeed perform a vital function in the fusion of the primary palate, we would expect to see the formation of a cleft, or at least consistent delay in fusion of the beaks in anophthalmic embryos. However, we show here that craniofacial prominence fusion is rather robust (despite the high proportion of cleft lip and palate incidence in humans). These results also provide some insight into the evolution of mammals, since reduction in eye size is shown to occur without disturbing the structural integrity of the upper jaw, revealing a possible path to smaller eye evolution in embryonic mammals without the imposition of a serious risk of clefting. That said, minor changes in size, shape, and position of the prominences were observed, which later manifested into effects on the developing skull. However, through geometric morphometric analysis, we showed that the effects of the eyes on the skull were localized to the orbital regions and did not compromise overall shape of the upper jaw when anophthalmia was bilateral. The above findings add to the understanding of the interaction between the components of craniofacial development, which should lead to a better understanding of the immense morphological diversity exhibited by the amniote clade.

4. Materials and Methods

4.1. Embryo Acquisition, Staging, and Eye Ablation

All animal work was performed following guidelines from the University of Michigan Animal Care and Use program. Fertile white leghorn chicken (*Gallus gallus*) eggs were obtained from the Michigan State University Poultry Teaching & Research Center and incubated in our laboratory at 38.0 $^{\circ}$C. Embryos were staged according to (Hamburger and Hamilton, 1951). At day 2.5 of incubation (stage 15) eggs were windowed using standard procedures. Between stages 16 - 18, embryos were stained with 0.5% neutral red (Sigma) to help with visibility. Ablation of the entire eye was then performed using fine microdissection forceps either on the exposed right eye for unilateral ablation, or both eyes for bilateral ablation. A second set of unilateral eye ablation surgeries were performed at stages 13-14. Control samples were windowed and stained with 0.5% neutral red, but otherwise left untreated. Embryos at stage 41 were euthanized by decapitation *in ovo* before harvesting. Mouse embryos (B6C3F1 strain) were purchased from Embryotech Laboratories, Inc. (Haverhill, MA, USA) as specimens fixed in 70% ethanol.

4.2. MicroCT Scanning Conditions

Specimens were harvested and fixed in 4% paraformaldehyde (PFA) overnight, followed by dehydration in ethanol concentration series up to 70%. Specimens were then transferred to 1% phosphomolybdic acid (PMA) for 48 hours before being embedded in 75% agarose for scanning (n=14 – stage 28 chicken; n=5 – stage 29 chicken; n=4 – E13 mouse). Samples were then placed in a 19 mm diameter specimen holder and scanned over the entirety of the head using a microCT system (µCT100 Scanco Medical, Bassersdorf, Switzerland). Scan settings were: voxel size 10 µm, 70 kVp, 114 µA, 0.5 mm AL filter, integration time of 500 ms, and 1500 projections.

4.3. Eye and Prominence Segmentation

Relative eye size was analyzed for normal stage 28 (n=4) and stage 29 (n=4) chicken embryos and E12 (n=2) and E13 mouse embryos (n=4). These stages were specifically chosen due to prominence fusion taking place during this time. MicroCT scan .vff files were uploaded to MicroView (Parallax Innovations Inc., Ilderton, ON, Canada), reoriented and isosurfaces rendered in 3D. Subsequently, files were saved as .vtk files and uploaded to 3D Slicer v. 4.2.2 (open-source software, http://www.slicer.org) for segmentation. The left and right eyes were

segmented separately in each specimen. Due to interspecific differences in overall head size, we quantified eye size as an eye:head volumetric ratio. In chicken and mouse, entire heads were segmented from the top of the head to the lower border of the mandible, including the eyes. A paired t-test was performed to compare the relative size between the left and right eye within each sample for both chickens and mice. An independent sample t-test was used to compare relative eye size between chicken and mouse. Eye:head volumetric proportions were calculated for each individual eye per sample specimen. Since there were no statistically significant differences in size found between the left and right eye of each sample, the graph in Fig. 2 shows average eye:head measurements from 8 eyes per species from four specimens each of chicken and mouse. All figures were compiled using Adobe Photoshop CS4 and Adobe Illustrator CS4 (Adobe Systems, Inc.).

For craniofacial prominence segmentation, unilateral anophthalmia-induced n=5 stage 28 and stage 29 chicken embryos were scanned using microCT, and left and right lateral nasal and maxillary, and globular prominences were segmented using the same software and conditions as eye segmentation. Roundness of maxillary prominence was quantified using ImageJ (NIH, Bethesda, MD), within the Shape Descriptors plugin. Prominence cross sections from stage 29 embryos (n=3) were isolated using Adobe Photoshop CS4 and separated into cranial (closest to lateral nasal prominence), middle, and caudal thirds, each section was then scored for roundness. Subsequently, values were averaged within each third and compared using a two-tailed t-test in Microsoft Excel. Maxillary prominence and globular process volumes were calculated in stage 28 embryos (n=5) using 3D Slicer v. 4.2.2 (open-source software, http://www.slicer.org).

4.4. Bone and Cartilage Staining

Stage 41 embryos were harvested, washed in a 1 x phosphate buffered saline (PBS) and fixed in 100% ethanol for a minimum of 4 days. After fixation, embryos were stained for bone and cartilage according to (Plant et al., 2000). Following fixation, samples were skinned, remaining eyes removed, and permeabilized with acetone for 4 days. Subsequently, samples were stained in a solution of 5% acetic acid, 0.015% Alcian blue and 0.005% Alizarin red in 70% ethanol for 7 days on a shaker. Heads were then cleared for 48 hours in 2% KOH in water, and then transferred to a 2% KOH/20% glycerol solution for several weeks until completely cleared.

Solution changes were made every two days. Cleared samples were stored and photographed in a 50% glycerol solution, imaged using a Leica dissecting microscope with a SPOT RT_{SE} Camera and SPOT 5.2 software (Diagnostic Instruments Inc.).

4.5. Morphometric Analysis

Landmark-based two-dimensional geometric morphometrics was performed on cleared and stained skulls using 29 (x,y) landmarks on the palatal view (Fig. 6, Table 2), digitized by the same person (JJ) with tpsDig2 v. 2.31 (Rohlf, 2018). Three phenotypes were analyzed: untreated controls (n=24), unilateral anophthalmia (n=20), and bilateral anophthalmia (n=22). Landmark coordinates of the entire dataset (n=66) were subjected to covariance analyses in MorphoJ software v. 1.07 (Klingenberg, 2011). Statistical analyses were performed in R v.3.3.3. (R Development Core Team, 2016) with the *rmorph* package (Baylac, 2012) and *mass* library (Venables and Ripley, 2013). Size of each landmark configuration was estimated as its centroid size (Dryden and Mardia, 1993). Landmark configurations were superimposed with a generalized Procrustes fit in order to extract shape variables (Dryden and Mardia, 1993; Klingenberg et al., 2002; Rohlf and Slice, 1990). Due to object symmetry in our data, two covariance matrices were generated corresponding to symmetric and asymmetric components of shape variation. The asymmetric component was then utilized for all shape analyses (Klingenberg, 2015). Principal Component Analysis (PCA) was performed to find patterns in the relationships among groups, as well as to explore the major axes and features of shape variation (Baylac and Frieß, 2005; Jolliffe, 1986; Klingenberg et al., 2002). Canonical Variate Analysis (CVA), which unlike PCA assumes a priori knowledge of group membership, was used to explore best distinguishing shape features among the three phenotypes. CVA also quantified morphological differentiation in terms of pairwise Procrustes distances between the groups, which measure the absolute magnitude of shape deviation (Klingenberg and Monteiro, 2005). Statistical significance of the Procrustes distances resulted from permutation tests with 10,000 permutation iterations per comparison (Good, 1994; Klingenberg, 2011). Discriminant Function Analysis (DFA) was used to visualize shape dissimilarities between pairs of group means.

In order to test size variation of the total palatal area among the three phenotypes, represented by the area enclosed by the outline connecting the 13 most peripheral landmarks (#1-2-10-14-18-28-

26-27-29-19-15-11-3-1), a one-way analysis of variance (ANOVA) was used, taking size as the dependent variable and phenotype as the independent variable. In order to characterize change in the size of the remaining eye in unilaterally ablated individuals, the size of the palatal area below the remaining (left) eye, delimited by landmarks #11-15-19-29-23-21-7-11, was compared to that of the controls using a one-way ANOVA.

Surface areas of palatal bones were measured by first disarticulating the bones from the skull (n=5), and subsequently imaging them in approximately the same position as their original shape. Pterygoid bones were not disarticulated since they proved difficult to realign to equivalent surface areas.

Table 2. Description of landmarks used for morphometric analysis

Landmark	Description
1	Anterior edge of premaxilla, at midline
2 & 3	Anterior-most tip of maxilla
4 & 5	Posterior-most point of intersection between premaxilla and palatine
6 & 7	Posterolateral-most point of intersection between maxilla and palatine
8 & 9	Posteromedial-most point of maxilla
10 & 11	Posterior-most edge of premaxilla
12 & 13	Anterior-most point of protrusion on the palatine
14 & 15	Anterior-most point of intersection between maxilla and jugal
16 & 17	Anteromedial-most tip of palatine
18 & 19	Posterior-most point of intersection between jugal and quadratojugal
20 & 21	Anterolateral-most point of pterygoid
22 & 23	Posterolateral-most point of pterygoid
24 & 25	Anteromedial-most point of quadrate
26 & 27	Posterolateral-most point of quadrate
28 & 29	Posterior-most tip of quadratojugal

Acknowledgements

We would like to thank Michelle Lynch for assistance with microCT scan optimization. Specimens were scanned at the University of Michigan School of Dentistry MicroCT Core funded in part by NIH/NCRR S10RR026475-01. J.A. is a member of the Michigan Integrative Musculoskeletal Health Core Center (MiMHC) and as such, research reported in this publication was supported by the National Institute of Arthritis and Musculoskeletal and Skin Diseases of the National Institutes of Health under Award Number P30 AR069620. The content is solely the responsibility of the authors and does not necessarily represent the official views of the National Institutes of Health. J.J. wrote the manuscript, performed eye surgeries, and performed clearing/staining and morphometric analysis of skulls. J.M.-V. performed morphometric analysis of skulls. S.E. performed eye segmentation and volume analysis. N.H. performed craniofacial prominence segmentation. J.A. was responsible for project design, Fig. preparation, eye surgeries, clearing and staining, segmentation, statistical analyses, and co-writing of the manuscript. Additional funding was also provided by startup funds from the University of Michigan-Dearborn to J.A.

Author Contributions

Conceptualization and Methodology, J.A.; Segmentation and volumetric measurement of eyes, S.E.; Segmentation and analysis of craniofacial prominences, N.H.; Morphometric analysis and methodology, J.M.-V. and J.J.; Writing – Original Draft Preparation, J.J. and J.A; Writing – Review & Editing, J.J., J.M.-V., JA, S.E., N.H.; Supervision, J.A.; Project Administration, J.A.

Conflict of Interest

The authors declare that there are no conflicts of interest.

References

Abramyan, J. and Richman, J.M., 2015. Recent insights into the morphological diversity in the amniote primary and secondary palates. Dev Dyn. 244, 1457-68.

Abramyan, J., Thivichon-Prince, B. and Richman, J.M., 2015. Diversity in primary palate ontogeny of amniotes revealed with 3D imaging. J Anat. 226, 420-33.

Akbareian, S.E., Pitsillides, A.A., Macharia, R.G. and McGonnell, I.M., 2015. Occipital foramina development involves localised regulation of mesenchyme proliferation and is independent of apoptosis. J Anat. 226, 560-74.

Apt, L. and Isenberg, S., 1973. Changes in orbital dimensions following enucleation. Arch Ophthalmol. 90, 393-5.

Bardakjian, T.M. and Schneider, A., 2011. The genetics of anophthalmia and microphthalmia. Curr Opin Ophthalmol. 22, 309-13.

Baumel, J.J. and Witmer, L.M., 1993. Osteologia, Nuttall Ornithological Club, Cambridge, MA.

Baylac, M., 2012. Rmorph: A R geometric and multivariate morphometrics library. Available from the author (baylac@mnhn.fr).

Baylac, M. and Frieß, M., 2005. ourier descriptors, Procrustes superimposition, and data dimensionality: an example of cranial shape analysis in modern human populations. , Springer, Boston, MA.

Bellairs, A., 1955. Skull development in chick embryos after ablation of one eye. Nature. 176, 658-9.

Bininda-Emonds, O.R., Jeffrey, J.E. and Richardson, M.K., 2003. Is sequence heterochrony an important evolutionary mechanism in mammals? Journal of Mammalian Evolution. 10, 335-361.

Clark, J.M., Welman, J., Gauthier, J.A. and Parrish, J.M., 1993. The laterosphenoid bone of early archosauriforms. Journal of Vertebrate Paleontology. 13, 48-57.

Coulombre, A.J. and Crelin, E.S., 1958. The role of the developing eye in the morphogenesis of the avian skull. Am J Phys Anthropol. 16, 25-37.

Couly, G., Creuzet, S., Bennaceur, S., Vincent, C. and Le Douarin, N.M., 2002. Interactions between Hox-negative cephalic neural crest cells and the foregut endoderm in patterning the facial skeleton in the vertebrate head. Development. 129, 1061-73.

Couly, G., Grapin-Botton, A., Coltey, P., Ruhin, B. and Le Douarin, N.M., 1998. Determination of the identity of the derivatives of the cephalic neural crest: incompatibility between Hox gene expression and lower jaw development. Development. 125, 3445-59.

De Beer, G.R., 1937. The Development of the Vertebrate Skull., Clarendon Press, Oxford.

Dixon, M.J., Marazita, M.L., Beaty, T.H. and Murray, J.C., 2011. Cleft lip and palate: understanding genetic and environmental influences. Nat Rev Genet. 12, 167-78.

Dryden, I.L. and Mardia, K.V., 1993. Multivariate shape analysis. Sankhyā: The Indian Journal of Statistics, Series A. 460-480.

Dufton, M., Hall, B.K. and Franz-Odendaal, T.A., 2012. Early lens ablation causes dramatic long-term effects on the shape of bones in the craniofacial skeleton of Astyanax mexicanus. PLoS One. 7, e50308.

Eames, B.F. and Schneider, R.A., 2008. The genesis of cartilage size and shape during development and evolution. Development. 135, 3947-58.

Fish, J.L., Sklar, R.S., Woronowicz, K.C. and Schneider, R.A., 2014. Multiple developmental mechanisms regulate species-specific jaw size. Development. 141, 674-84.

Foster, F.S., Zhang, M., Duckett, A.S., Cucevic, V. and Pavlin, C.J., 2003. In vivo imaging of embryonic development in the mouse eye by ultrasound biomicroscopy. Invest Ophthalmol Vis Sci. 44, 2361-6.
Good, P., 1994. Permutation tests: A practical guide to resampling methods for testing hypotheses, Springer, New York.
Goodall, N., Kisiswa, L., Prashar, A., Faulkner, S., Tokarczuk, P., Singh, K., Erichsen, J.T., Guggenheim, J., Halfter, W. and Wride, M.A., 2009. 3-Dimensional modelling of chick embryo eye development and growth using high resolution magnetic resonance imaging. Experimental eye research. 89, 511-521.
Gundlach, K.K., Guthoff, R.F., Hingst, V.H., Schittkowski, M.P. and Bier, U.C., 2005. Expansion of the socket and orbit for congenital clinical anophthalmia. Plast Reconstr Surg. 116, 1214-22.
Hamburger, V. and Hamilton, H.L., 1951. A series of normal stages in the development of the chick embryo. Journal of Morphology. 88, 49-92.
Hogg, D.A., 1978. The articulations of the neurocranium in the postnatal skeleton of the domestic fowl (Gallus gallus domesticus). J Anat. 127, 53-63.
Jeffery, J.E., Bininda-Emonds, O.R., Coates, M.I. and Richardson, M.K., 2002. Analyzing evolutionary patterns in amniote embryonic development. Evol Dev. 4, 292-302.
Jiang, R., Bush, J.O. and Lidral, A.C., 2006. Development of the upper lip: morphogenetic and molecular mechanisms. Dev Dyn. 235, 1152-66.
Jolliffe, I.T., 1986. Principal component analysis. Spring-verlag, New York. 2:29.
Kim, J.S., Min, J., Recknagel, A.K., Riccio, M. and Butcher, J.T., 2011. Quantitative three-dimensional analysis of embryonic chick morphogenesis via microcomputed tomography. Anat Rec (Hoboken). 294, 1-10.
Klingenberg, C., 2015. Analyzing fluctuating asymmetry with geometric morphometrics: concepts, methods, and applications. Symmetry. 7, 843-934.
Klingenberg, C.P., 2011. MorphoJ: an integrated software package for geometric morphometrics. Mol Ecol Resour. 11, 353-7.
Klingenberg, C.P., Barluenga, M. and Meyer, A., 2002. Shape analysis of symmetric structures: quantifying variation among individuals and asymmetry. Evolution. 56, 1909-20.
Klingenberg, C.P. and Monteiro, L.R., 2005. Distances and directions in multidimensional shape spaces: implications for morphometric applications. Syst Biol. 54, 678-88.
Landauer, W., 1938. Notes on cross-beak in fowl. Journal of Genetics. 37, 51-68.
Lee, S.H., Bedard, O., Buchtova, M., Fu, K. and Richman, J.M., 2004. A new origin for the maxillary jaw. Dev Biol. 276, 207-24.
Llorente-Gonzalez, S., Peralta-Calvo, J. and Abelairas-Gomez, J.M., 2011. Congenital anophthalmia and microphthalmia: epidemiology and orbitofacial rehabilitation. Clin Ophthalmol. 5, 1759-65.
MacDonald, M.E., Abbott, U.K. and Richman, J.M., 2004. Upper beak truncation in chicken embryos with the cleft primary palate mutation is due to an epithelial defect in the frontonasal mass. Dev Dyn. 230, 335-49.
Neath, P., Roche, S.M. and Bee, J.A., 1991. Intraocular pressure-dependent and -independent phases of growth of the embryonic chick eye and cornea. Invest Ophthalmol Vis Sci. 32, 2483-91.

Ng, D., Hadley, D.W., Tifft, C.J. and Biesecker, L.G., 2002. Genetic heterogeneity of syndromic X-linked recessive microphthalmia-anophthalmia: is Lenz microphthalmia a single disorder? Am J Med Genet. 110, 308-14.
Parsons, T.E., Schmidt, E.J., Boughner, J.C., Jamniczky, H.A., Marcucio, R.S. and Hallgrimsson, B., 2011. Epigenetic integration of the developing brain and face. Dev Dyn. 240, 2233-44.
Plant, M.R., MacDonald, M.E., Grad, L.I., Ritchie, S.J. and Richman, J.M., 2000. Locally Released Retinoic Acid Repatterns the First Branchial Arch Cartilages in Vivo. Developmental Biology. 222, 12-26.
Richman, J.M. and Tickle, C., 1989. Epithelia are interchangeable between facial primordia of chick embryos and morphogenesis is controlled by the mesenchyme. Dev Biol. 136, 201-10.
Rohlf, F.J., 2018. TpsDig2, digitize coordinates of landmarks and capture outlines [software version 2.31]. State University of New York. Available at: http://life.bio.sunysb.edu/ee/rohlf/software.html.
Rohlf, F.J. and Slice, D., 1990. Extensions of the Procrustes method for the optimal superimposition of landmarks. Systematic Biology. 39, 40-59.
Sarnat, B.G. and Shanedling, P.D., 1974. Increased orbital volume after periodic intrabulbar injections of silicone in growing rabbits. Am J Anat. 140, 523-31.
Schneider, R.A., 2018. Neural crest and the origin of species-specific pattern. Genesis. 56, e23219.
Schneider, R.A. and Helms, J.A., 2003. The cellular and molecular origins of beak morphology. Science. 299, 565-8.
Sun, D., Baur, S. and Hay, E.D., 2000. Epithelial-mesenchymal transformation is the mechanism for fusion of the craniofacial primordia involved in morphogenesis of the chicken lip. Dev Biol. 228, 337-49.
Thompson, H., Griffiths, J.S., Jeffery, G. and McGonnell, I.M., 2010. The retinal pigment epithelium of the eye regulates the development of scleral cartilage. Dev Biol. 347, 40-52.
Tucker, A.S. and Lumsden, A., 2004. Neural crest cells provide species-specific patterning information in the developing branchial skeleton. Evol Dev. 6, 32-40.
Tucker, S.M., Sapp, N. and Collin, R., 1995. Orbital expansion of the congenitally anophthalmic socket. Br J Ophthalmol. 79, 667-71.
Uz, E., Alanay, Y., Aktas, D., Vargel, I., Gucer, S., Tuncbilek, G., von Eggeling, F., Yilmaz, E., Deren, O., Posorski, N. and Ozdag, H., 2010. Disruption of ALX1 causes extreme microphthalmia and severe facial clefting: expanding the spectrum of autosomal-recessive ALX-related frontonasal dysplasia. The American Journal of Human Genetics. 86, 789-896.
Venables, W.N. and Ripley, B.D., 2013. Modern applied statistics with S-PLUS, Springer Science & Business Media.
Wedden, S.E., 1987. Epithelial-mesenchymal interactions in the development of chick facial primordia and the target of retinoid action. Development. 99, 341-51.
Williamson, K.A. and FitzPatrick, D.R., 2014. The genetic architecture of microphthalmia, anophthalmia and coloboma. Eur J Med Genet. 57, 369-80.

Yamamoto, Y., Espinasa, L., Stock, D.W. and Jeffery, W.R., 2003. Development and evolution of craniofacial patterning is mediated by eye-dependent and -independent processes in the cavefish Astyanax. Evol Dev. 5, 435-46.

Supplementary Fig. S1.

The premaxilla, maxillary, palatine bones were disarticulated from specimens (n=5) and surface area measured. Pterygoids were measured in-situ since they were clearly visible and proved to be difficult to place in equivalent positions once disarticulated

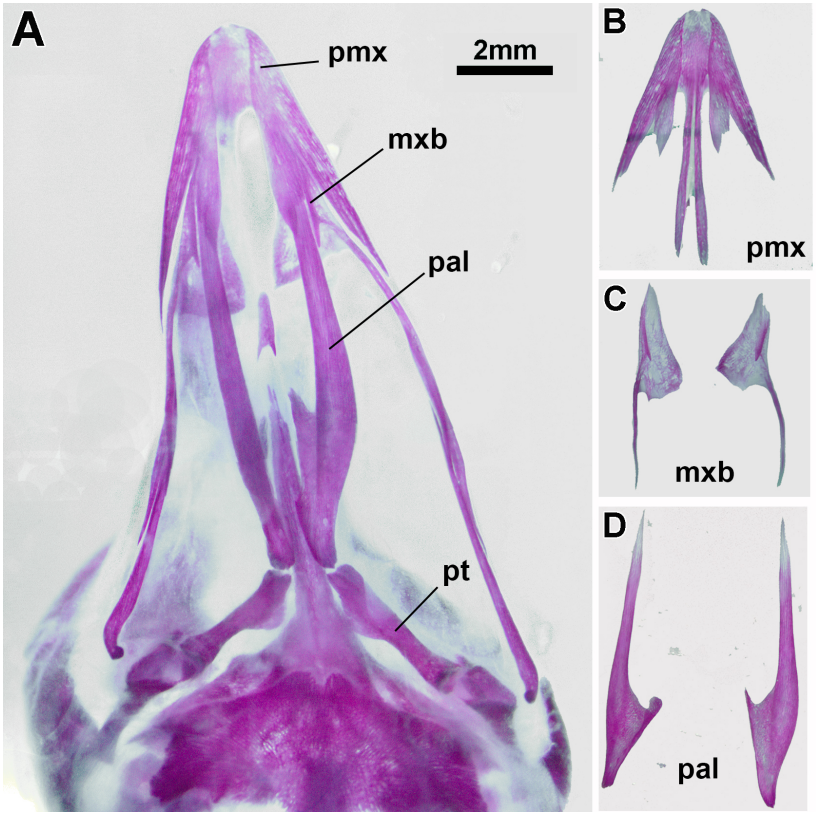

Supplementary Table S1

Surface area ratios of MICROPHTHALMIC : CONTROL sides				
Specimen ID	**Maxillary**	**Palatine**	**Premaxillary**	**Pterygoid**
HH2	0.864554164	0.919255695	1.021122343	0.852081183
JA-300	1.259830501	0.968422504	0.933901382	0.908487838
JA-125	1.107074956	0.834263632	0.967716465	0.910198333
JA-128	1.203008411	0.869010587	1.058503754	0.84320293
JJ20	0.977549569	0.846534263	0.940961408	0.925490997
P-values	0.24623366	**0.012989055**	0.49776119	**0.008820052**

* P Value – two tailed paired t-test